



Section 1. Clinical medicine

DOI: 10.29013/EJBLS-24-3-3-20



FIRST-IN-CLASS SMALL MOLECULE BTLA INHIBITORS AS POTENTIAL CANCER THERAPIES

Brian Kuo¹

¹ Cupertino High School

Cite: Kuo B. (2024). *First-In-Class Small Molecule Btla Inhibitors as Potential Cancer Therapies*. *The European Journal of Biomedical and Life Sciences 2024, No 3* <https://doi.org/10.29013/EJBLS-24-3-3-20>

Abstract

Modern cancer treatments have developed to a great extent – however, various factors such as cancer types and resistance continue to make effective treatments difficult to create for many cancers. Among different cancer treatments, immunotherapy shows promise because of its utilization of one's own body's immune system in fighting off cancerous cells. Immune checkpoints instruct the body to stop producing anti-cancer cells, and blocking these checkpoints can be effective in reactivating an immune system. B and T Lymphocyte Attenuator (BTLA) is an immune checkpoint that shows promise as an immunotherapy target, but current clinical trials focus solely on large monoclonal antibodies that can have severe side effects and other limitations due to larger molecular size. By identifying small molecule BTLA inhibitors, the development of anti-cancer immunotherapy treatments could be vastly improved. In this paper I utilize a variety of experiments to virtually screen small molecules and identify potential BTLA inhibitors. First, I located suitable binding sites in BTLA using 3 different methods (geometric, energetic, and machine learning methods). I identified compounds using virtual screening in two different experiments, by identifying HVEM B-chain pharmacophore maps, then scanning the ZINC compound library for matches. Then, I verified the compounds' site binding on BTLA with molecular docking in SwissDock. Finally, the druggability of the remaining compounds were evaluated twice, for drug properties and for toxicity, in SwissADME and ProTox 3.0 respectively. In the end, two promising compounds with favorable energetic interactions with BTLA, strong drug properties according to Lipinski's rule, and low toxicity were identified as drug candidates for different applications, which hold potential for being pivotal milestones in the field of cancer therapy.

Keywords: *B and T Lymphocyte Attenuator (BTLA), immunotherapy, cancer, cancer therapy, immune checkpoints, drug discovery, small molecule inhibitor*

Introduction

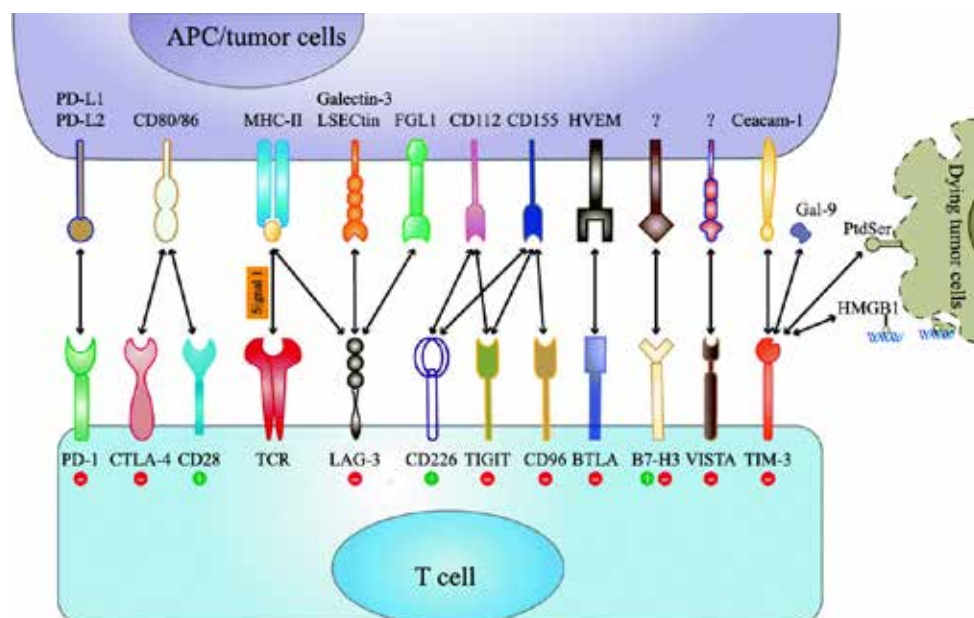
Cancer, a disease caused by uncontrolled, abnormal cell growth, is becoming more prominent of a global issue than ever, and with it comes human ingenuity in discovering cancer treatments. Modern treatments range from chemotherapy, which utilizes chemicals to kill dividing cancer cells, to radiation therapy, which induces damage to the DNA of cancer cells using radiation (Hossain *et al.*, 2023; Jaffray *et al.*, 2015). In addition, scientists have found that combining multiple treatments can be effective at an affordable cost (Bayat Mokhtari *et al.*, 2017). However, the large variability in different cancer types, cancer resistance to drugs, and the side effects of toxic drugs continue to make universal treatments nigh impossible (Barot *et al.*, 2023).

Among different types of cancer treatments, immunotherapy utilizes one's own body's immune system to fight off cancer. Currently, a better understanding of the immune system and immune surveillance has slowly made immunotherapy more viable – however, it is still a juvenile cancer treatment

due to the difficulty of predicting its effectiveness and toxicity (Esfahani *et al.*, 2020). But compared to conventional treatment methods such as chemotherapy, which can see harmful damage to parts of the human body that aren't cancerous, immunotherapy could potentially have fewer side effects (Shahid *et al.*, 2019).

Immune checkpoints allow the immune system to keep itself in check – they can inhibit or stimulate molecules, allowing the immune system to either attenuate or activate T-cell proliferation and activity. Immune checkpoints are necessary in maintaining homeostasis in the immune system, and to prevent any collateral damage done by one's own immune system. Because of its regulatory nature, some cancers have been found to slip under an immune system and halt T-cell proliferation through immune checkpoint pathways. On the other hand, immune checkpoints can be blocked in order to activate T-cells, which can target cancers (Lee *et al.*, 2016). The function of immune checkpoint pathways and our ability to inhibit them mark a promising avenue in immuno-oncology.

Figure 1. Various immune checkpoints found on T-cells, and their binding counterparts found on antigen-presenting or tumor cells (Qin *et al.*, 2019)



Inhibitors for immune checkpoints PD-1 and CTLA-4 are currently the forefront of immunotherapy, having received FDA approval (Zhang *et al.*, 2021). However, the inhibitors for these pathways are limited – immune checkpoint monotherapies for PD-1 and

CTLA-4 have been found to show responses in only 20%-30% of patients (Padmanee *et al.*, 2021). In addition, various cancers currently exhibit complete resistance to the current treatment methods (Pilard *et al.*, 2021). Because of this, research of newer inhibitors

for immune checkpoints could mean great strides in the field of cancer treatment.

B and T Lymphocyte Attenuator (BTLA), is an immune checkpoint most commonly found on B and T lymphocytes and dendritic cells, and negatively regulates immune responses to maintain immune homeostasis when bound with Herpesvirus Entry Mediator (HVEM), which is found on similar cells (Sedy *et al.*, 2005; Ning *et al.*, 2021). Similarly to PD-1 and CTLA-4, BTLA's negatively regulatory nature in the immune system means it is involved in many immune disorders and immune system functions (Watanabe *et al.*, 2003). For example, mice have been found to have a greater risk of autoimmune diseases when deficient of BTLA (Oya *et al.*, 2008).

BTLA on T-cells inhibits activity when activated by HVEM, which can prevent T-cells from being able to fight against cancer cells. Since cells deficient in BTLA are found to have increased T-cell activity and proliferation, inhibiting BTLA could potentially be pursued as an immunotherapy target (Andrzejczak *et al.*, 2024). However, the current main molecule for inhibiting BTLA is the monoclonal antibody (mAb) icatolimab, which was approved for clinical trials in 2019. Its larger size may provide challenges for immunotherapy in the future, such as longer lasting side effects and lower maneuverability, highlighting a need for discovering new, viable BTLA inhibitors that are of smaller molecular sizes.

Method

Locating Suitable Binding Sites on BTLA

Before beginning to find small molecules that could bind to BTLA, possible binding locations must first be identified. This was done using 3 different methods, all utilizing BTLA's Protein Database (PDB) Code: 1XAU. This code represents the 3D structure of BTLA when it is not interacting with external molecules, which gives a strong base to identify binding sites for the use of small molecule binding.

Geometric Method

The aim of the geometric method was to find binding sites on BTLA that are the right size for small molecules to target. First, the PDB code 1XAU was typed into the web structure-based modeling server, proteins.plus, to identify the

correct BTLA model (Schöning-Stierand *et al.*, 2022). Then, the geometric based binding sites were calculated using the default parameters of DoGSiteScorer, which detected binding sites based solely on the 3D structure of BTLA (Volkamer *et al.*, 2010).

Energetic-based Method

The second method was the energetic-based method using FTSite at ftsitesite.bu.edu, which identified binding sites using multiple molecular probes that account for charge and energy at the binding sites (Kozakov *et al.*, 2015). BTLA's PDB code was entered into FTSite, where the job was queued, completed, and later viewable on the website.

Machine Learning Method

The last method used to identify suitable binding sites on BTLA was the machine learning method, using prankweb.cz (Jakubec *et al.*, 2022). This method uses a variety of factors, from geometric to energetic, to identify binding sites. To use the model, the PDB code for BTLA was entered and submitted.

Virtual Screening with Pharmacophore

In order to narrow down suitable compounds to bind with BTLA and prevent its binding with HVEM, a virtual screening process must be undergone. First pharmacophore maps were identified with PocketQuery, then the ZINC library was screened with ZINCPharmer. Pharmacophore maps utilized the PDB code 2AW2, and were of the B-chain of HVEM, representing the interaction between BTLA and HVEM.

Pharmacophore Mapping

To identify the best pharmacophore maps on the BTLA/HVEM interaction, I used pocketquery.csb.pitt.edu. The PDB code 2AW2 was entered and searched, and the clusters with the highest scores on the B-chain were used. The B-chain is the HVEM side of the interaction, and using these maps will enable the discovery of small compounds that mimic its interaction with BTLA. The maps were then exported to ZINCPharmer through the website's in-built export function.

Small Molecule Virtual Screening

In zincpharmer.csb.pitt.edu, the pharmacophore maps were isolated by hiding the ligand and receptor residues in the viewer tab. Then, the submit query button scanned and identified matching compounds from

the ZINC library, which were then organized from lowest to highest Root Mean Square Deviation (RMSD) score to pick the best compound matches based on the pharmacophore map.

Molecular Docking

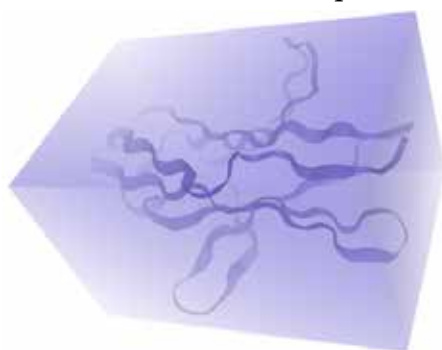
In order to quantify the energy between 20 chosen compounds and different bind-

ing sites on BTLA, I used molecular docking using the newest version of swissdock.ch. For each ligand, the SMILES format is found with the ZINC library website, and the PDB code for BTLA, 1XAU, was used. To define the search space, the sizes shown in Table 1 were used. Parameters were set to the default of 1.

Table 1. Search space used for molecular docking of BTLA in SwissDock experiment

Search box center (Å)	30	28	14
Search box size (Å)	28	25	41

Figure 2. Search space used for BTLA in the SwissDock experiment



Drug Properties Evaluation using SwissADME

With the top 5 compounds from the molecular docking experiment, I utilized swissadme.ch to evaluate the drug properties of the molecules. The respective SMILES were entered into the website and the evaluations were run. I looked at the 4 elements of Lipinski's rule as well as water solubility, GI absorption, and BBB permeability to evaluate the drug effectiveness of these compounds.

Toxicity Prediction using ProTox 3.0

The purpose of the toxicity prediction experiment is to see if the toxicity of the two remaining compounds are within an acceptable

toxicity range. This was done using Tox Prediction from ProTox 3.0, where the SMILES format and all models were selected. I then compared the predicted values (LD50, toxicity class, etc) as well as the predicted active elements and models between the two compounds to determine drugging suitability.

Results

Geometric Method

Results

Figure 3. Six suitable binding sites on BTLA, color labeled, based on geometric methods and identified using the DoGSiteScorer

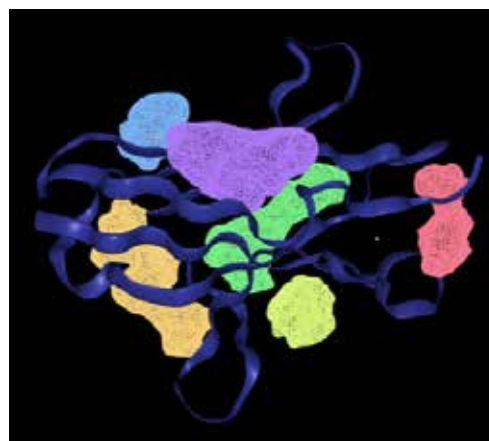


Table 2. Volume, Surface Area, and Drug Score assigned to each binding site with the Geometric method, using DoGSiteScorer at proteins. plus

Name	Volume (Å ³)	Surface Area (Å ²)	Drug Score
P_0 (Orange)	323.84	479.33	0.62
P_1 (Violet)	243.01	322.2	0.42
P_2 (Lime Green)	184.51	439.5	0.58
P_3 (Red)	121.98	306.51	0.36
P_4 (Blue)	113.98	326.8	0.21
P_5 (Green)	103.68	242.98	0.17

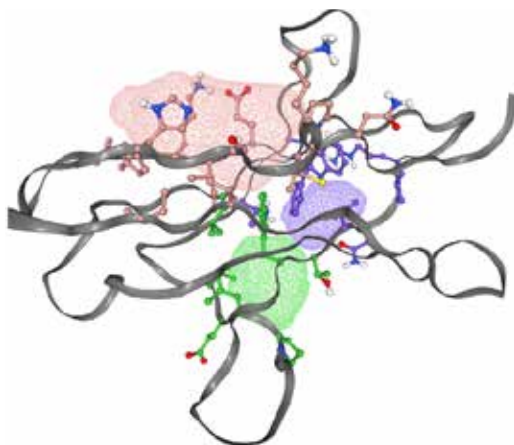
Discussion

Using the geometric method, 6 binding sites were identified with Protein.plus (DoGSiteScorer), each with varying volumes (103.68 to 323.84 Å³) and surface areas (242.98 to 479.33 Å²). The top binding site (P_0) in BTLA (PDB: 1XAU) based on Protein.plus had a volume of 323.84 Å³ and surface area of 479.33 Å². This binding site is highlighted in orange in Figure 3. Because Protein.plus is only based on the 3D shape of BTLA and not any other factors, such as the energetic ability of small molecules to bind at the site, there are more binding sites than testing with other methods.

Energetic-Based Method

Results

Figure 4. Three suitable binding sites, color labeled, identified based on the energetic-based method, using FTSite



Discussion

From the energetic-method tested using FTSite, 3 suitable binding sites were identified,

labeled in pink, green, and purple. These represent binding sites on BTLA (PDB: 1XAU) that are more energetically-favorable for small compounds to potentially bind to.

Machine Learning Method

Results

Figure 5. First suitable binding site of BTLA (labeled in red) based on the machine learning method, identified using PrankWeb

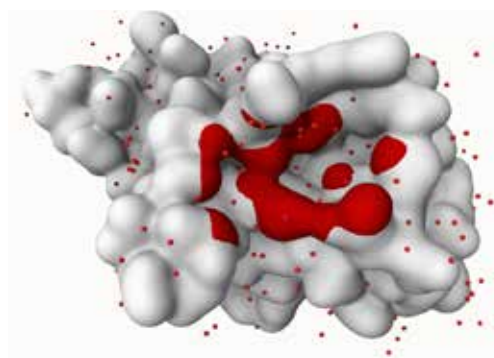


Figure 6. Second suitable binding site of BTLA (labeled in yellow) based on the machine learning method, identified using PrankWeb

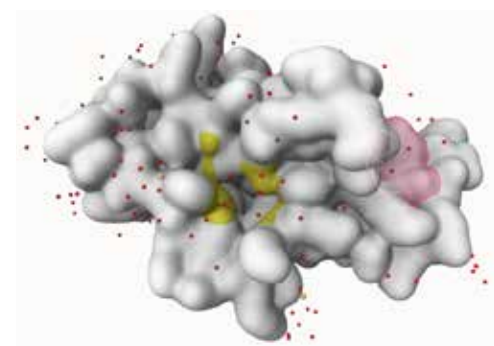


Table 3. Suitable binding site rankings, drug scores, and residue information for the two binding site results from the machine learning method, using PrankWeb

Binding Site Ranking	Drug Score	# of Residues	Residues
1 (red)	2.58	10	LYS50 ASN52 VAL 57 PRO 58 LEU59 GLU60 LEU65 HIS86 SER88 ASP 89

Binding Site Ranking	Drug Score	# of Residues	Residues
2 (yellow)	1.08	9	ILE17 LYS18 SER21 HIS23 LYS32 ILE33 GLU34 PRO 36 VAL 109

Discussion

The machine learning method shows two suitable binding sites, fewer than the other two methods used, because it combines a variety of factors instead of using just one. The binding sites must fit structural, physico-chemical, and evolutionary factors – the stricter criteria means that fewer sites are

selected (Kufareva I., Abagyan R. 2012). The top binding site identified with PrankWeb (labeled as red in Figure 4) has a drug score of 2.58 and consists of 10 amino acid residues.

Pharmacophore Mapping

Results

Table 4. PocketQuery pharmacophore mapping results for top five scoring clusters on the B chain of HVEM (Koes et al, 2012)

Ranking	Score	Distance (Å)	Size (residues)	Residues
1	0.771762	9.1795	3	GLU31 LEU32 GLY34
2	0.754979	7.298	2	LEU32 GLY34
3	0.731909	0	1	LEU32
4	0.730782	9.1795	4	GLU31 LEU32 THR33 GLY34
5	0.726755	11.9219	4	PRO 17 GLU31 LEU32 GLY34

Figure 7. Top PocketQuery match for HVEM B-chain

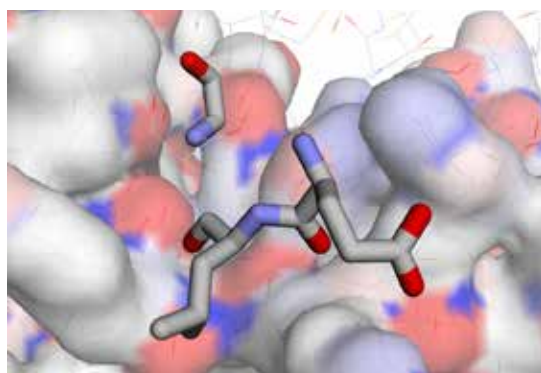


Figure 8. Second top PocketQuery match for HVEM B-chain

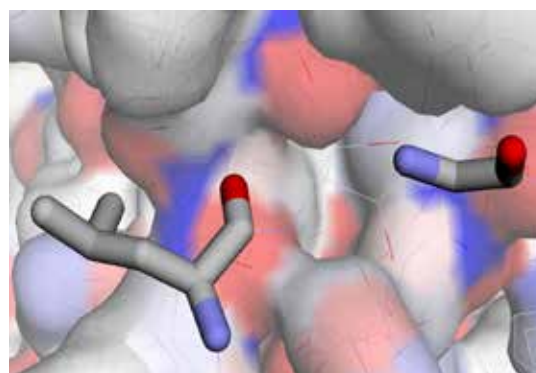
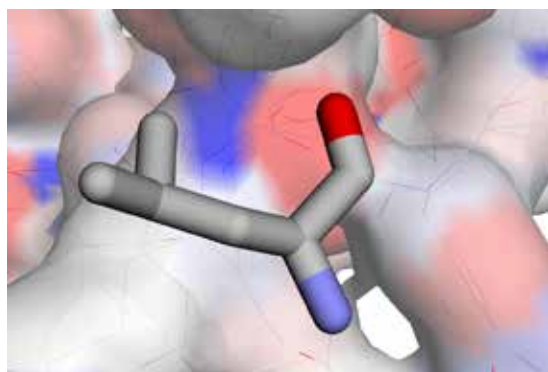


Figure 9. Third top PocketQuery match for HVEM B-chain



Discussion

PocketQuery search results for the BTLA/HVEM complex (PDB code: 2AW2) on the B chain showed the highest scoring results (with higher score being suitability for the design of small molecule inhibitors) generally having the residues GLU31, LEU32, and GLY34. The top five best scoring clusters for the B chain had varying distances (7.298 to 11.9219 Å) and sizes (1 to 4 residues), with

the best scoring cluster having a distance of 9.1795 Å and size of 3.

Small Molecule Virtual Screening Results

Figure 10. Pharmacophore map for top PocketQuery match



Figure 11. Pharmacophore map for top PocketQuery match after isolating 3 closest interactions



Table 5. Top compound match results from ZINCPharmer for highest scoring pharmacophore map of HVEM B-chain (Koes et al., 2012)

Name	RMSD Score	Mass (daltons)	Residue Binds
ZINC37452229	0.013	288	6
ZINC38148338	0.016	560	8
ZINC34781361	0.017	494	15
ZINC38867909	0.018	224	5

Table 6. Highest scoring pharmacophore map overlaid with compounds that showed lowest RMSD scores in ZINCPharmer

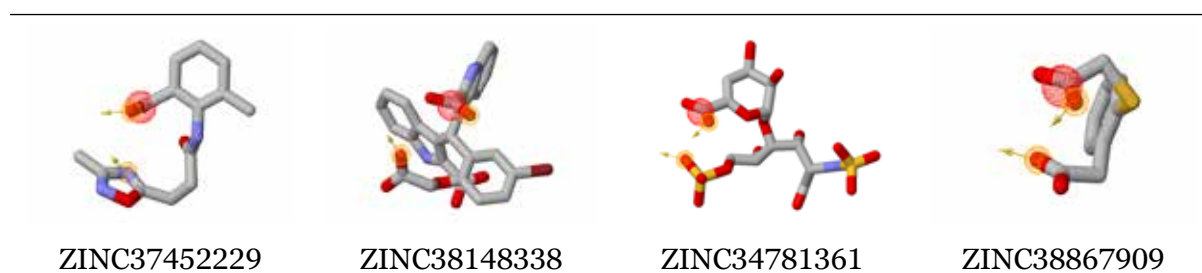


Figure 12. Pharmacophore map for second top PocketQuery match



Table 7. Top compound match results from ZINCPharmer for second highest scoring pharmacophore map of HVEM B-chain

Name	RMSD Score	Mass (daltons)	Residue Binds
ZINC49601555	0.008	445	15
ZINC93485320	0.009	289	6
ZINC83429713	0.011	463	13
ZINC83429714	0.011	463	13
ZINC06624253	0.011	414	10
ZINC12664461	0.011	414	10
ZINC39223733	0.012	360	14
ZINC81245051	0.012	316	9

Table 8. Second highest scoring pharmacophore map overlaid with compounds that showed lowest RMSD scores in ZINCPharmer

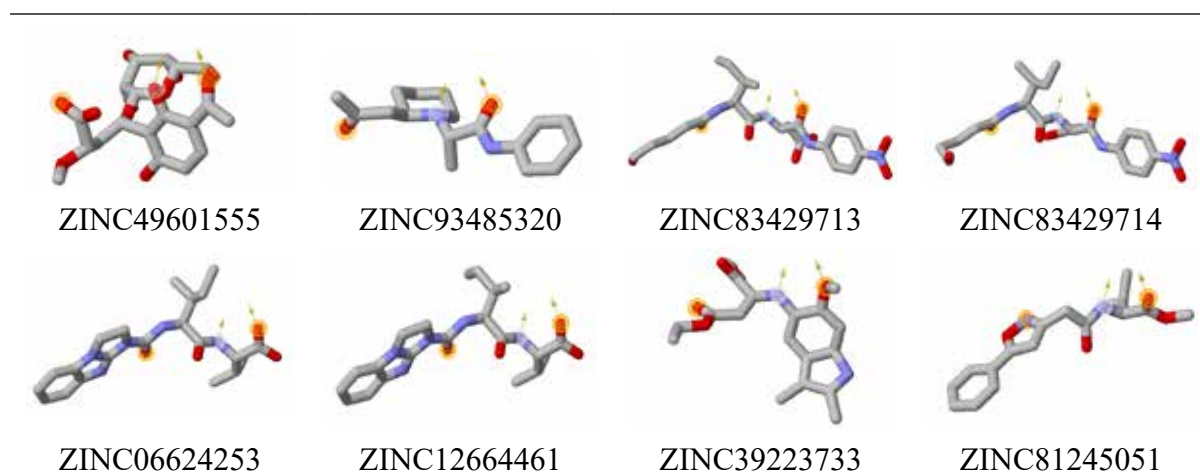
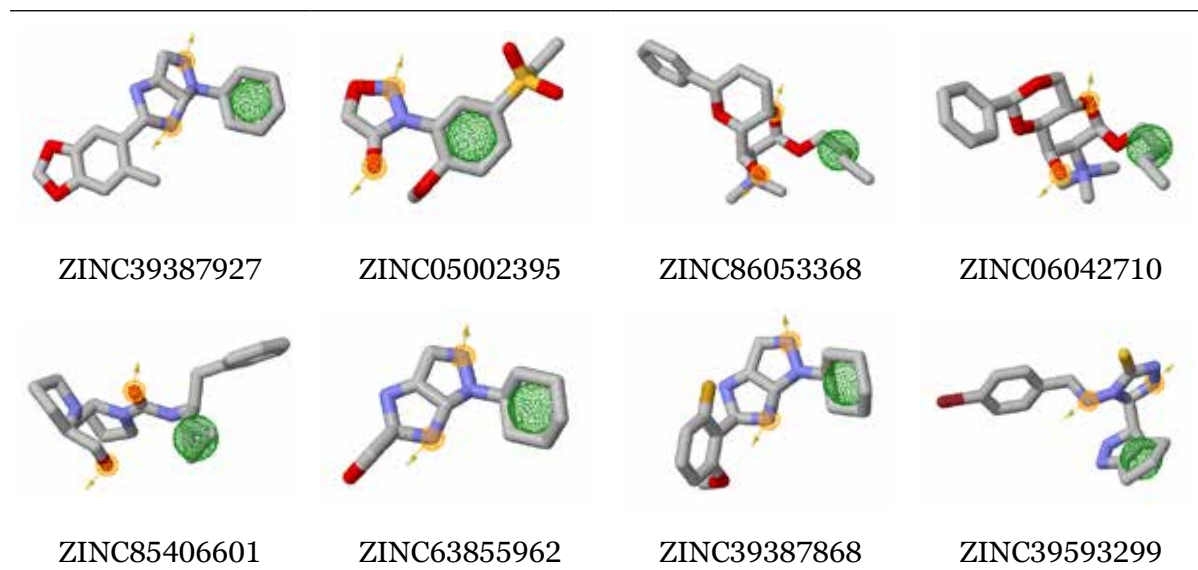


Figure 13. Pharmacophore map for third top PocketQuery match

Table 9. Top compound match results from ZINCPharmer for third highest scoring pharmacophore map of HVEM B-chain

Name	RMSD Score	Mass (daltons)	Residue Binds
ZINC39387927	0.008	326	3
ZINC05002395	0.009	286	7
ZINC86053368	0.009	364	11
ZINC06042710	0.010	366	11
ZINC85406601	0.011	373	8
ZINC63855962	0.012	258	2
ZINC39387868	0.012	316	4
ZINC39593299	0.012	390	3

Table 10. Third highest scoring pharmacophore map overlaid with compounds that showed lowest RMSD scores in ZINCPharmer



Discussion

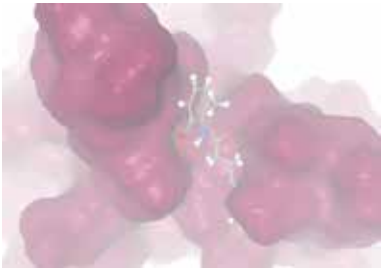
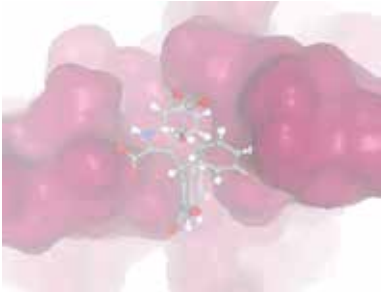
The RMSD values signal level of deviation the molecule has from the pharmacophore map (Kufareva *et al.*, 2012). Out of the 20 selected compounds with low RMSD values, from 3 different pharmacophore maps of the B chain on the BTLA-HVEM complex, there were varying masses (224 to 560) and residue binds (2 to 15). The compounds with the

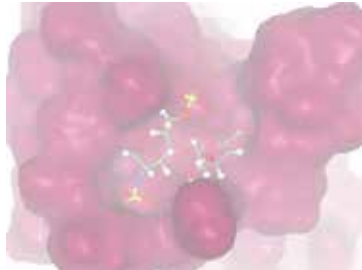
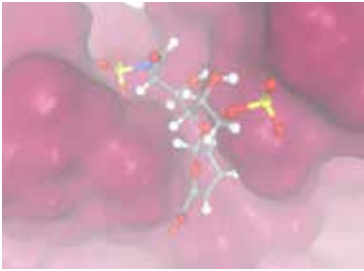
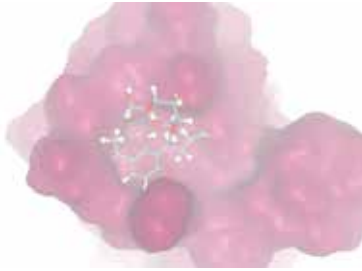

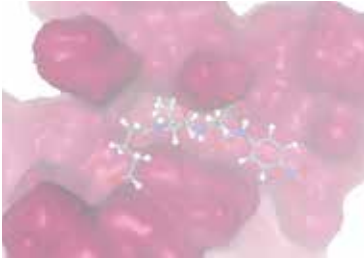
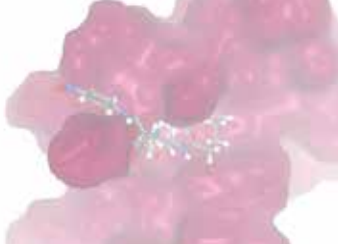
lowest RMSD values were ZINC49601555 and ZINC39387927 with RMSD values of 0.008. Masses for the compounds were 445 and 326 daltons respectively, and the compounds had residue binds of 15 and 3.

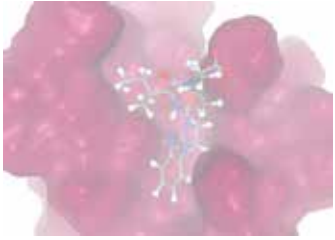
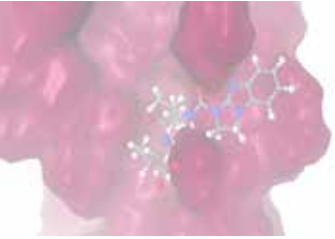
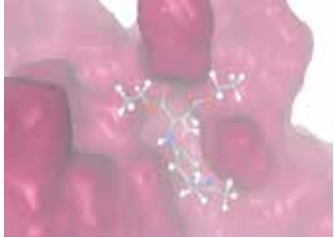
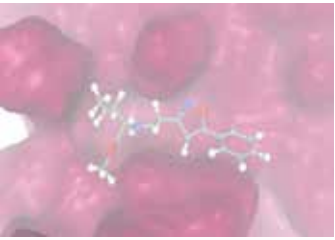



Molecular Docking

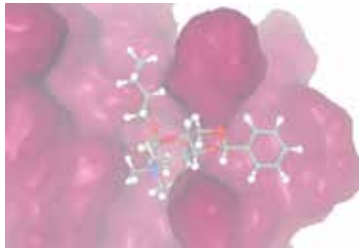
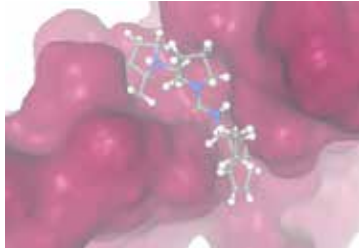

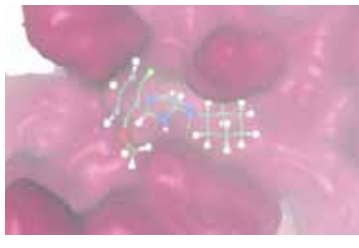
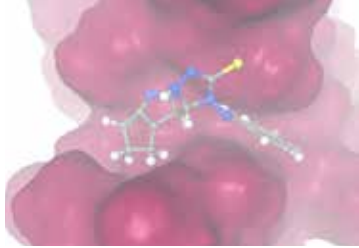
Results

Table 11. Molecular docking results for the 20 compounds with lowest RMSD scores, using the updated version of Swiss Dock.ch.

Compound	Highest SwissParam Score (kcal/mol)	Highest SwissParam Cluster	Highest Interaction
ZINC37452229	-6.6440	1	
ZINC38148338	-6.5126	13	

Compound	Highest SwissParam Score (kcal/mol)	Highest SwissParam Cluster	Highest Interaction
ZINC34781361	-6.5749	27	
ZINC38867909	-7.0349	3	
ZINC49601555	-6.8794	0	
ZINC93485320	-6.7812	1	
ZINC83429713	-7.1073	3	
ZINC83429714	-7.4917	2	

Compound	Highest SwissParam Score (kcal/mol)	Highest SwissParam Cluster	Highest Interaction
ZINC06624253	-7.0473	0	
ZINC12664461	-7.1827	0	
ZINC39223733	-7.2914	9	
ZINC81245051	-7.1301	4	
ZINC39387927	-7.3083	0	
ZINC05002395	-6.7593	4	
ZINC86053368	-6.5743	9	

Compound	Highest SwissParam Score (kcal/mol)	Highest SwissParam Cluster	Highest Interaction
ZINC06042710	-6.7704	0	
ZINC85406601	-7.1930	0	
ZINC63855962	-7.2660	0	
ZINC39387868	-7.4206	1	
ZINC39593299	-7.2100	0	

Discussion

Out of the 20 selected compounds, 12 compounds were able to achieve a SwissParam score of below -7 kcal/mol. The highest SwissParam scores for each compound ranged from -6.5126 to -7.4917 kcal/mol, with the top 5 compounds according to score being ZINC83429714, ZINC39387868, ZINC39387927, ZINC39223733, and ZINC63855962, from highest to lowest score. The SwissParam score

represents free energy, so these 5 compounds with the largest numerical scores have the most optimal energy interactions. The locations of these interactions were on clusters 2, 1, 0, 9, and 0 respectively.

Drug Properties Evaluation Results

Table 12. Drug properties of top 5 compounds, identified with SwissADME

Compound	Hydrogen Bond Donors (<5)	Hydrogen Bond Acceptors (<10)	Calculated LogP (1–5)	Mass (<500 daltons)	Lipinski's rule violations	Water Solubility ESOL (moderate or more)	GI Absorption (high)	BBB Permeability (no)
ZINC83429714	3	8	2.11	463.46	0	–2.10 (Soluble)	Low	No
ZINC39387868	1	5	3.19	316.37	0	–3.69 (Soluble)	High	Yes
ZINC39387927	1	5	2.99	326.39	0	–3.88 (Soluble)	High	Yes
ZINC39223733	1	6	4.06	360.40	0	–2.89 (Soluble)	High	No
ZINC63855962	1	4	2.51	258.32	0	–2.76 (Soluble)	High	No

Discussion

After evaluating all 5 compounds, the two molecules that successfully pass the set benchmarks for druggability were ZINC39223733 and ZINC63855962. Both of these molecules fit the elements of Lipinski's rule (<5 H bond donors, <10 H bond acceptors, 1–5 CLogP, <500 daltons) as well as being soluble, having High GI absorption and

not being BBB permeable. ZINC39387868 and ZINC39387927 also passed Lipinski's rule, and were soluble with high GI absorption. However, they are BBB permeable, potentially posing risks of side effects.

Toxicity Prediction*Results***Table 13.** Predicted Toxicity Data using Tox-Prediction from Pro Tox 3.0.

Compound	LD50 (mg/kg)	Toxicity Class	Toxic Elements
ZINC39223733	187	3	Nephrotoxicity Respiratory Toxicity Nutritional Toxicity
ZINC63855962	800	4	Neurotoxicity Respiratory Toxicity Carcinogenicity BBB-barrier Eco Toxicity Clinical Toxicity

Figure 14. Toxicity Radar Chart for Compound ZINC39223733, showing active toxic areas in nutritional, respiratory, and nephrotoxicity, lower than the average of its class of FDA-approved drugs

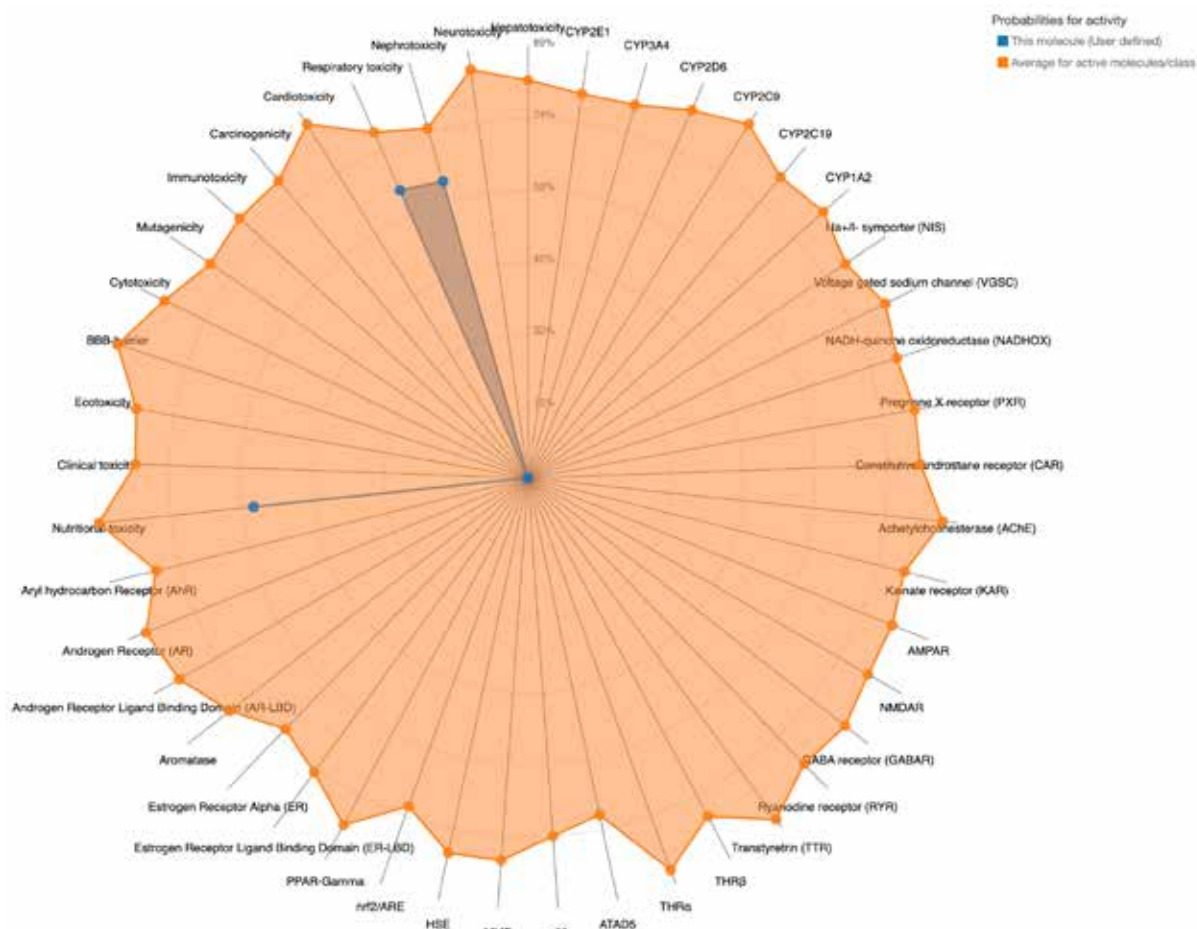
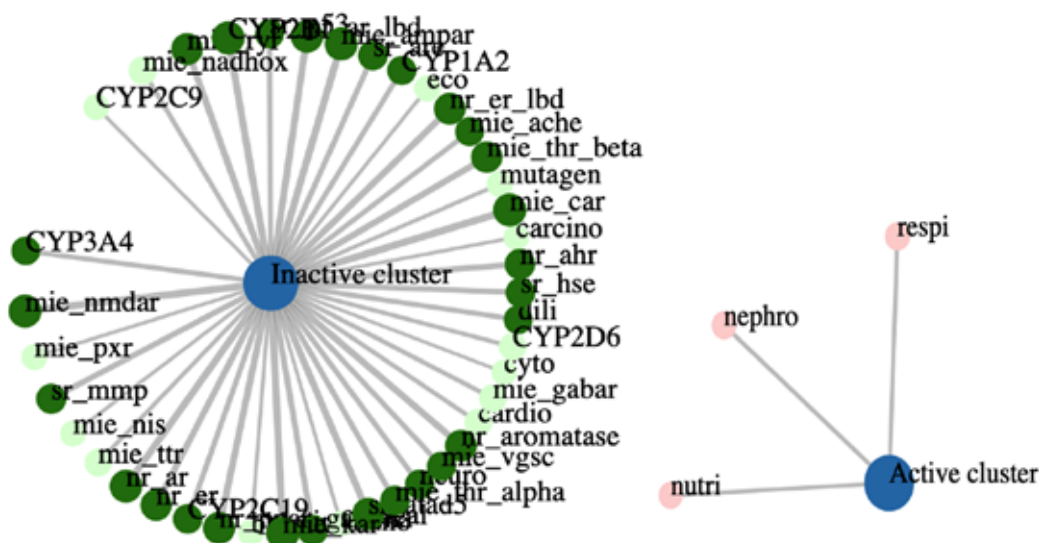


Figure 15. Network Charts for Compound ZINC39223733, showing the active and inactive clusters from the ProTox 3.0 experiment



Discussion

Screening both compounds with the toxicity prediction method found that ZINC39223733 was the better drug candidate, with a lower LD50 of 187 mg/kg and toxicity class of 3, but fewer active toxic elements. As seen in Figure 14, the 3 active toxic elements of ZINC39223733 were all within an acceptable range.

ZINC63855962 had a higher LD50 of 800 mg/kg and toxicity class of 4 – however, it had a total of 6 toxic elements, with 2 elements, the blood-brain barrier and respiratory toxicity elements, being slightly above the average FDA-approved drug of its class.

Comparing the two drug candidates, ZINC39223733 stands out as a better candidate overall because of its fewer toxic elements. On the other hand, ZINC63855962's ability to penetrate the blood-brain barrier means it could be used to target tumors in the brain, which is only made possible because of the compound's BBB permeability.

Statement of Limitations

The main limitation of these experiments is that they are virtual, and may not reflect accurate real-life test results for binding and toxicity. Going forward, *in vitro* or *in vivo* experiments should be performed to evaluate the effectiveness of the compounds as BTLA inhibitors. Another limitation is that the PrankWeb evaluation of the first experiment only resulted in two binding sites on BTLA. PrankWeb was the most accurate binding site evaluator of the three methods used because it included the most factors, which brings up limitations for the ability of compounds to bind to BTLA. Finally, another limitation was in the Molecular Docking experiment, where many of the selected top 20 compounds had SwissParam scores above -7 kcal/mol, which were not ideal for moving into the drug property evaluation. This meant less compounds in the final drug and toxicity evaluation stages, which could have cut down on the number of promising compounds identified.

Conclusion

The first experiment identified two main binding sites on BTLA that accounted for all three binding site testing methods. In the next experiment, PocketQuery identified pharmacophore maps for molecules from the Zinc compound library to bind to, of which three maps were selected. From these three maps, I used ZincPharmer to select 20 of the best compounds with the lowest RMSD scores on these maps. In the third experiment, I used molecular docking in SwissDock to compare the binding efficacy of the 20 compounds, and the top five compounds for numerical SwissParam score were selected. These five compounds were evaluated for drug properties in the SwissADME experiment, where two passed Lipinski's rule as well as additional drug property factors. In the last experiment, ProTox 3.0 identified both of these final two compounds, ZINC39223733 and ZINC63855962 as suitable drug targets due to acceptable LD50s and low number of active clusters. Between the two, ZINC39223733 is a better candidate overall, with less toxic elements – this choice is also backed by its lower SwissParam score of -7.4206 kcal/mol, compared to ZINC63855962's score of -7.2660 kcal/mol. On the other hand, ZINC63855962's blood-brain barrier permeability shows potential for use in treatment of brain tumors. Ultimately, this research has concluded two promising compounds for small molecule BTLA inhibitors as potential cancer therapies.

Going forward, the next steps would involve biophysical interactions with BTLA, to overcome the uncertainty of virtual model interactions. In the long term, these inhibitors can be tested in animal studies and eventually clinical trials. By doing so, the effectiveness of these two top compounds, ZINC39223733 and ZINC63855962, as BTLA inhibitors can be evaluated, bringing the field to cancer immunotherapy a new ray of hope

References

- Hossain M. B., Haldar Neer A. H. Chemotherapy. *Cancer Treat Res.* 2023; 185: 49–58.
Jaffray D. A., Gospodarowicz M. K. Radiation Therapy for Cancer. In: Gelband H., Jha P., San-
karanarayanan R., Horton S., editors. *Cancer: Disease Control Priorities, Third Edition*

- (Volume 3). Washington (DC): The International Bank for Reconstruction and Development / The World Bank; 2015.– Nov 1. Chapter 14.
- Bayat Mokhtari R., Homayouni T.S., Baluch N., Morgatskaya E., Kumar S., Das B., Yeger H. Combination therapy in combating cancer. *Oncotarget*. 2017. Jun 6; 8(23): 38022–38043.
- Barot S., Patel H., Yadav A., Ban I. Recent advancement in targeted therapy and role of emerging technologies to treat cancer. *Med Oncol*. 2023. Oct 7; 40(11): 324.
- Esfahani K., Roudaia L., Buhlaiga N., Del Rincon S.V., Papneja N., Miller W.H. Jr. A review of cancer immunotherapy: from the past, to the present, to the future. *Curr Oncol*. 2020. Apr; 27 (Suppl 2): S87–S97.
- Shahid K., Khalife M., Dabney R., Phan A. T. Immunotherapy and targeted therapy – the new roadmap in cancer treatment. *Ann. Transl. Med*. 2019; 7. Doi: 10.21037/ATM.2019.05.58. 595–595.
- Lee L., Gupta M., Sahasranaman S. Immune Checkpoint inhibitors: An introduction to the next-generation cancer immunotherapy. *J Clin Pharmacol*. 2016. Feb; 56(2): 157–69.
- Zhang H., Dai Z., Wu W., Wang Z., Zhang N., Zhang L., Zeng W.J., Liu Z., Cheng Q. Regulatory mechanisms of immune checkpoints PD-L1 and CTLA-4 in cancer. *J Exp Clin Cancer Res*. 2021. Jun 4; 40(1): 184.
- Padmanee Sharma, Bilal A. Siddiqui, Swetha Anandhan, Shalini S. Yadav, Sumit K. Subudhi, Jianjun Gao, Sangeeta Goswami, James P. Allison; The Next Decade of Immune Checkpoint Therapy. *Cancer Discov* 1 April 2021; 11 (4): 838–857.
- Pilard C., Ancion M., Delvenne P., Jerusalem G., Hubert P., Herfs M. Cancer immunotherapy: it's time to better predict patients' response. *Br J Cancer*. 2021. Sep; 125(7): 927–938.
- Sedy J.R., Gavrieli M., Potter K. G., Hurchla M.A., Lindsley R. C., Hildner K., et al. B and T lymphocyte attenuator regulates T cell activation through interaction with herpesvirus entry mediator. *Nat Immunol*. 2005; 6(1): 90–8.
- Ning Z., Liu K., Xiong H. Roles of BTLA in Immunity and Immune Disorders. *Front Immunol*. 2021. Mar 29; 12: 654960.
- Watanabe N., Gavrieli M., Sedy J.R., Yang J., Fallarino F., Loftin S. K., et al. BTLA is a lymphocyte inhibitory receptor with similarities to CTLA-4 and PD-1. *Nat Immunol*. 2003; 4(7): 670–9.
- Oya Y., Watanabe N., Owada T., Oki M., Hirose K., Suto A., et al. Development of autoimmune hepatitis-like disease and production of autoantibodies to nuclear antigens in mice lacking B and T lymphocyte attenuator. *Arthritis Rheum*. 2008; 58(8): 2498–510.
- Andrzejczak, A., Karabon, L. BTLA biology in cancer: from bench discoveries to clinical potentials. *Biomark Res* 12, 8 (2024).
- Qin, S., Xu, L., Yi, M. et al. Novel immune checkpoint targets: moving beyond PD-1 and CTLA-4. *Mol Cancer* 18, 155. (2019).
- Schöning-Stierand, K., Diedrich, K., Ehrt, C., Flachsenberg, F., Graef, J., Sieg, J., Penner, P., Poppinga, M., Ungethüm, A., Rarey, M. (2022). ProteinsPlus: a comprehensive collection of web-based molecular modeling tools. *Nucleic Acids Research*, 50: W611–W615.
- Volkamer, A., Griewel, A., Grombacher, T., Rarey, M. Analyzing the topology of active sites: on the prediction of pockets and subpockets. *J Chem Inf Model* 2010. 50 (11), 2041–52.
- Kozakov D., Grove L. E., Hall D. R., Bohnuud T., Mottarella S. E., Luo L., Xia B., Beglov D., Vajda S. The FT Map family of web servers for determining and characterizing ligand-binding hot spots of proteins *Nature Protocols* 2015. 10(5): 733–755.
- Dávid Jakubec, Petr Škoda, Radoslav Krivák, Marian Novotný and David Hoksza. PrankWeb 3: accelerated ligand-binding site predictions for experimental and modelled protein structures. *Nucleic Acids Research*. May, 2022.
- David Ryan Koes, Carlos J. Camacho, Small-molecule inhibitor starting points learned from protein–protein interaction inhibitor structure, *Bioinformatics*,– Volume 28.– Issue 6. March 2012.– P. 784–791.

David Ryan Koes, Carlos J. Camacho, ZINCPharmer: pharmacophore search of the ZINC database, *Nucleic Acids Research*,– Volume 40.– Issue W1. 1 July, 2012, P. W409–W414.
Kufareva I., Abagyan R. Methods of protein structure comparison. *Methods Mol Biol.* 2012; 857: 231–57.

submitted 14.08.2024;
accepted for publication 31.08.2024;
published 29.10.2024
© Kuo B.
Contact: mrkuo787@gmail.com